FMR/EPR study of samples obtained by nitriding and nitrides reduction of nanocrystalline iron

J. Typek[1], N. Guskos[1,2], G. Zolnierkiewicz[1], A. Guskos[1], A. Kielbasa[3] and W. Arabczyk[3]

[1]Institute of Physics, West Pomeranian University of Technology, Szczecin, Al. Piastow 48, 70-311 Szczecin, Poland.
[2]Department of Solid State Physics, Faculty of Physics, University of Athens, Panepistimiopolis, 15 784 Zografos, Athens, Greece.
[3]Institute of Inorganic Chemical Technology and Environmental Engineering, West Pomeranian University of Technology, Pulaskiego 10, 70-322 Szczecin, Poland

The aim of the study

The aim of this study was to determine the phase content of samples taken at different stages of nitriding and nitrides reduction of nanocrystalline iron, using only FMR/EPR spectra of these samples taken at room temperature. The obtained results will be compared and discussed with previously carried out XRD measurements on these samples. Moreover, some magnetic characteristics of these phases revealed in studied samples will be determined.

Sample preparation

Recrystallisation of nanocrystalline iron occurs at temperatures higher than 300°C thus the material was promoted with aluminum and calcium oxides to prevent that undesirable effect. Mixture containing magnetite and small amounts of aluminum and calcium oxides was fused at 1600°C. After melting and cooling, prepared frozen lava was crumbled (grains size of 1.0 – 1.2 mm) and polithermally reduced by hydrogen. As the result of the reduction iron with nanocrystalline structure was produced. Prepared nanocrystalline samples are pyrophoric thus that material has to be passivated to form a passive layer of iron oxide on the grain surface to prevent oxidation. Chemical composition of studied materials was determined by using inductively coupled plasma method (ICP – OES, Spectrometer Perkin Elmer, type Optima 5300DV). Apart from metallic iron, the samples contained the following oxides: 3.3 wt.% Al_2O_3, 2.8 CaO wt.%, 0.65 wt.% K_2O. The value of specific surface area was determined by means of Thermal Desorption method (AutoChem II 2920 apparatus by Micromeritics Company) and equals 12 m^2/g. XRD studies were carried out on the Phillips X'Pert PRO diffractometer (X – ray Diffraction apparatus with cooper lamp). An average size of iron nanocrystallites was determined by Scherrer's method and it was in 40-100 nm range. The obtained nanoparticles were strongly agglomerated.

The nitriding and the nitrides reduction processes

The nitriding process and the nitrides reduction process was investigated at the temperature of 400°C under atmospheric pressure. In the gas nitriding process, the nitriding potential is used to describe the nitridability of the nitriding atmosphere which contains ammonia. The nitriding potential is defined as $P \quad \frac{p_{NH_3}}{p_{H_2}^{3/2}}$, where p_{NH_3} and p_{H_2} are the partial pressures of the ammonia and hydrogen gases, respectively. In the nitriding process the nitriding potential was increasing. Inlet ratio of ammonia to hydrogen $\frac{X_{H2}}{X_{NH3}} \quad 0$ was changed when the stationary state was achieved. In that particular state only catalytic ammonia decomposition reaction are running.

After several hours, the mass of solid sample does not change therefore it allows to reach an equilibrium between gas and solid phases. Gas mixture composition was changing but the total gas load was constant (0.0025 $m^3\ s^{-1}\ kg^{-1}$). The values of partial pressure of gas reactants were determined on the basis of the results of the hydrogen content measurements as well as the material balance of the reactor. Studies of the reduction process of nitrides started up when the maximum nitriding degree of solid sample had reached (100% NH_3 let to the reactor). Decrease of nitriding potential was obtained by changing of gas phase composition until pure hydrogen was let to the reactor. During the reduction process stationary states exist as well. The relation between nitriding degree of solid sample and the nitriding potential exists in the stationary states during both processes. Different composition of solid sample at given nitriding potential is achieved, in respect to studied process: nitriding of iron or nitrides reduction.

On the basis of XRD studies the areas where phase composition of solid samples was changing during nitriding and reduction process were obtained. It was observed that during nitriding process the areas of various phases coexist in a wide range of nitriding potential. During the first phase of nitrading the observed nitriding level is relatively low and equals less than 0.015 mol_N/mol_{Fe}, what corresponds to the nitrogen dissolving and ammonia adsorption on the surface of iron; creation of solid solution of nitrogen in iron (α–Fe(N)). This is followed by formation of a new phase thus two phases exist simultaneously in the sample: α–Fe(N) and γ'–Fe_xN. On further nitrading stage only one phase exists - γ'–$Fe_{4-x}N$, where x decreases with the increase of the nitriding potential. After that continuation of saturating of the nitride by nitrogen causes two phases to exist simultaneously: γ'–$Fe_{4-x}N$ and ε–Fe_xN. It is followed by continuous saturating of the ε–Fe_xN by nitrogen.

Figure shows the dependence of nitrogen to α-iron concentration ratio on logarithm of nitrading potential. During nitriding of nanocrystalline iron and reduction of nanocrystalline nitrides as a function of potential, the hysteresis loop phenomenon is observed.

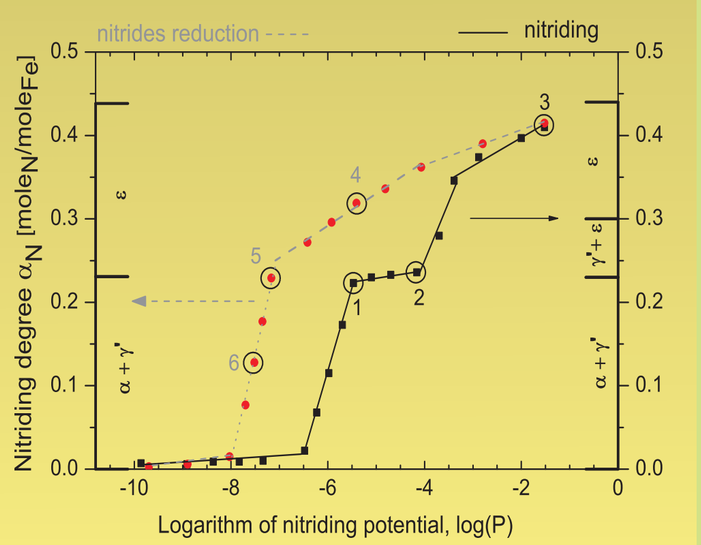

Figure 1. The dependence of nitriding degree on logarithm of the nitriding potential for the iron nitriding (solid line) and iron nitrides reduction (dashed line). Phase composition obtained from XRD measurements is indicated on both vertical axes.

FMR/EPR spectra

The registered magnetic resonance spectra of six studied samples were classified as EPR (sample 3) and FMR (samples 1-2, 4-6) spectra. EPR spectrum of paramagnetic ε–Fe_xN phase (at room temperature) was very weak in comparison of FMR spectra of ferromagnetic α –Fe(N) and γ'–$Fe_{4-x}N$ phases. Thus the paramagnetic resonance line of ε–Fe_xN phase can be only seen in sample 3 in which, according to XRD measurements, ferromagnetic α –Fe(N) and γ'–$Fe_{4-x}N$ phases were absent. In other samples strong ferromagnetic resonance line masked much weaker paramagnetic signal from ε–Fe_xN phase, even if that phase was detected by XRD (samples 2, 4 and 5).

EPR spectrum of sample 3 was fitted by two lines of lorentzian lineshape. The expression for the lorentzian lineshape (in absorption mode) as a function of the magnetic field is

$$P_{Lor} \quad \frac{P_{\max}}{1 \quad \frac{H \quad H_0}{0.5 \quad H}^2}$$

where P_{max} is the maximum power absorbed at resonance, H_0 is the resonance field and ΔH is the full width at half-maximum of the resonance line. These two lines represent parallel and perpendicular magnetic components of the anisotropy field of ε–Fe_xN phase.

FMR spectra of samples 1, 2, 4, 5, and 6 were fitted by four lines of dysonian lineshape each. Feher and Kip (Phys. Rev. 98, 337 (1955)) analyzed the shape of the resonance line using Dyson theory and applied it in case of low conductivity samples with a skin layer compared to the layer thickness. They obtained the following expression for the dysonian line

$$P_{Dys} \quad \frac{P_{Lor}}{2} \quad 1 \quad \frac{H \quad H_0}{0.5 \quad H}$$

Attempts to fit the FMR spectra with Callen lineshape components were unsuccessful because the obtained values of spectral parameters were unrealistic (resonance fields and linewidths greater than 20 kGs). FMR spectrum of each sample was successfully fitted with four component lines of dysonian lineshape. These lines were ascribed to the presence of two different phases in the sample (α –Fe(N) and γ'–$Fe_{4-x}N$). Two lines were attributed to each phase – these lines arise due to magnetic anisotropy, therefore they are parallel and perpendicular components of the anisotropy field.

Values of FMR/EPR spectra parameters

The parameters in Table 1 were calculated by the least-squares fitting of the sum of four/two Dysonian/Lorentzian components to the experimental FMR/EPR spectra.

The difference of resonance fields of both components (one in high H_H and the other in low field H_L) arising from the same phase could be correlated with the effective uniaxial anisotropy field H_a of that phaseby using the relation

$$H_a \quad \frac{2}{3} H_H \quad H_L$$

where H_H and H_L are the of high and low resonance fields arising from a particular phase. Calculated values of H_a for different phases in all investigated samples are presented in Table 2.

In Table 2 the relative integrated intensity ratio of α-Fe(N)/γ'-$Fe_{4-x}N$ phases calculated from FMR spectra is also shown. The integrated intensity of a particular phase is calculated as the sum of two similar terms (as there are two components for each phase): each term is a product of signal amplitude and the square of the linewidth, $I=A\cdot\Delta H^2$. It is supposed that the integrated intensity is proportional to concentration of the particular phase.

	Sample					
	1	2	3	4	5	6
Parameter	Dyson / Phase	Dyson / Phase	Lorentz / Phase	Dyson / Phase	Dyson / Phase	Dyson / Phase
A_1 [a.u.]	8.82	6.94	29.8	7.14	2.17	5.21
H_{01} [G]	285	262	3342	157	4773	3356
ΔH_1 [G]	3841	3896	323	4664	4196	6179
Phase	α-Fe(N)L	α-Fe(N)L	ε-Fe_xN_I	α-Fe(N)L	α-Fe(N)H	γ'-$Fe_{4-x}N_H$
A_2 [a.u.]	1.12	1.43	1.7	1.93	6.03	2.18
H_{02} [G]	4225	4559	2912	5258	3371	5302
ΔH_2 [G]	2603	3043	1959	3678	5017	5475
Phase	α-Fe(N)H	α-Fe(N)H	ε-Fe_xN_L	α-Fe(N)H	γ'-$Fe_{4-x}N_H$	α-Fe(N)H
A_3 [a.u.]	6.72	6.05		6.50	11.2	7.78
H_{03} [G]	1889	1919		2208	1385	1088
ΔH_3 [G]	4386	4542		5184	6490	5692
Phase	γ'-$Fe_{4-x}N_L$	γ'-$Fe_{4-x}N_L$		γ'-$Fe_{4-x}N_L$	γ'-$Fe_{4-x}N_L$	γ'-$Fe_{4-x}N_L$
A_4 [a.u.]	2.75	3.22		4.15	1.76	2.70
H_{04} [G]	3247	3412		3892	~0	43
ΔH_4 [G]	3268	3708		4368	2133	3002
Phase	γ'-$Fe_{4-x}N_H$	γ'-$Fe_{4-x}N_H$		γ'-$Fe_{4-x}N_H$	α-Fe(N)L	α-Fe(N)L

Table 1. Values of the FMR/EPR parameters (A – amplitude, H_0 – resonance field, ΔH – linewidth) for four components (two in case of sample 3) of the observed spectra. Each component has been attributed to a specific phase detected in XRD measurements. In each case (except for sample 3) the Dysonian lineshape of particular component was assumed. Subscripts L and H stand for low and high field components of a specific phase, respectively.

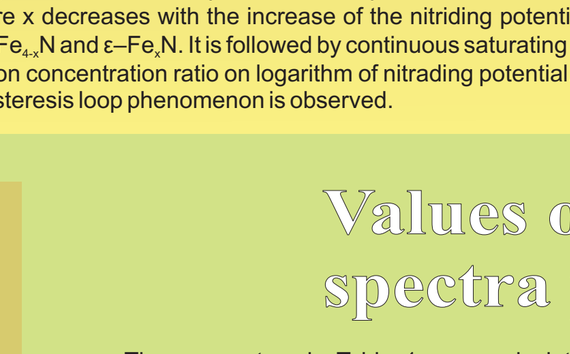

Figure 2. Experimental (symbols) and fitted (solid line) FMR spectra of samples 1-6.

		Sample					
		1	2	3	4	5	6
Effective uniaxial anisotropy field H_a [G]	Phase						
	α-Fe(N)	2627	2863	-	3401	3182	3506
	γ'-$Fe_{4-x}N$	905	995	-	1123	1324	1512
	ε-Fe_xN			287			
Relative integrated intensity ratio of α-Fe(N)/γ'-$Fe_{4-x}N$ phases from FMR spectra		0.86	0.70	-	0.71	0.08	0.20

Table 2. Values of the effective uniaxial anisotropy field of different phases in investigated samples and relative integrated intensity ratio of α-Fe(N)/γ'-$Fe_{4-x}N$ phases calculated from FMR spectra.

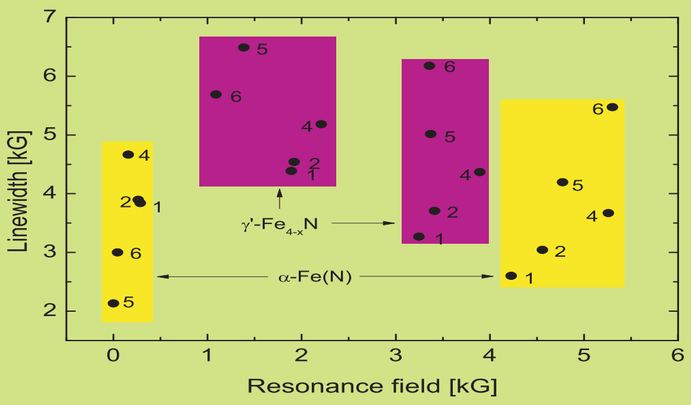

Figure 3. Graphical presentation of two spectral parameters (resonance field, linewidth) for each component in all investigated samples. Each rectangle collects components arising from the same phase.

Conclusions

- When paramagnetic and ferromagnetic phases are present in sample only lines from ferromagnetic phases will be observed in magnetic resonance spectra.
- For conducting samples the use of dysonian lineshape is better than Callen lineshape in fitting magnetic resonance spectra.
- The anisotropic FMR spectra of ferromagnetic Fe-N phases are correctly modelled by two components representing nanoparticles with their magnetization axes parallel and perpendicular to the external magnetic field. The effective uniaxial anisotropy field could be estimated from the separation of these both components.
- Magnetic anisotropy of α –Fe(N) phase is roughly three times bigger than of γ'–$Fe_{4-x}N$ phase
- The FMR/EPR measurements are in general in agreement with XRD results, although the relative amounts of detected phases might differ.
- During nitride reduction process the α –Fe(N) phase amount relative to the γ'–$Fe_{4-x}N$ phase is smaller than during nitriding process.